Expression of Two Human Skeletal Calcitonin Receptor Isoforms Cloned from a Giant Cell Tumor of Bone

The First Intracellular Domain Modulates Ligand Binding and Signal Transduction

Alan H. Gorn,* Sheila M. Rudolph,* Merrilee R. Flannery,* Cynthia C. Morton,§ Stanislawa Weremowicz,§ Jeng-Tzung Wang,* Stephen M. Krane,* and Steven R. Goldring*‡

**Department of Medicine, Harvard Medical School, Medical Services (Arthritis Unit), Massachusetts General Hospital, Boston, Massachusetts 02114; ‡Department of Medicine, New England Deaconess Hospital, Boston, Massachusetts 02115; and §Department of Pathology, Harvard Medical School, Brigham and Women's Hospital, Boston, Massachusetts 02115*

Abstract

Two distinct calcitonin (CT) receptor (CTR)-encoding cDNAs (designated GC-2 and GC-10) were cloned and characterized from giant cell tumor of bone (GCT). Both GC-2 and GC-10 differ structurally from the human ovarian cell CTR (o-hCTR) that we cloned previously, but differ from each other only by the presence (GC-10) or absence (GC-2) of a predicted 16-amino acid insert in the putative first intracellular domain. Expression of all three CTR isoforms in COS cells demonstrated that GC-2 has a lower binding affinity for salmon (s) CT (K_d ~ 15 nM) than GC-10 or o-hCTR (K_d ~ 1.5 nM). Maximal stimulatory concentrations of CT resulted in a mean accumulation of cAMP in GC-2 transfected cells that was greater than eight times higher than in cells transfected with GC-10 after normalizing for the number of receptor-expressing cells. The marked difference in maximal cAMP response was also apparent after normalizing for receptor number. GC-2 also demonstrated a more potent ligand-mediated cAMP response compared with GC-10 for both human (h) and sCT (the EC_{50} values for GC-2 were ~ 0.2 nM for sCT and ~ 2 nM for hCT; EC_{50} values for GC-10 were ~ 6 nM for sCT and ~ 25 nM for hCT). Reverse transcriptase PCR of GCT RNA indicated that GC-2 transcripts are more abundant than those encoding for GC-10. In situ hybridization on GCT tissue sections demonstrated CTR mRNA expression in osteoclast-like cells. We localized the human CTR gene to chromosome 7 in band q22. The distinct functional characteristics of GC-2 and GC-10, which differ in structure only in the first intracellular domain, indicate that the first intracellular domain of the CTR plays a previously unidentified role in modulating ligand binding and signal transduction via the G protein/adenylate cyclase system. (*J. Clin. Invest.* 1995. 95:2680–2691.) Key words: osteoclast • cyclic AMP • G protein • G protein–coupled receptor • chromosomal mapping

Introduction

Calcitonin (CT)[1] is a peptide hormone used clinically to treat disorders of bone remodeling, including osteoporosis, Paget's disease of bone, and hypercalcemia of malignancy. The skeletal actions of CT are mediated primarily by direct inhibition of osteoclastic bone resorption (1, 2). CT also exerts effects on nonskeletal organs. The CT receptor (CTR) has been identified in tissues such as kidney (1), brain (3, 4), lung (5), placenta (6), ovaries (7), testes (8), and spermatozoa (9). We previously cloned CTR cDNAs from libraries prepared from a porcine kidney cell line (10), a human ovarian cell line (7), and a mouse brain (11). Sequence analysis revealed that the CTR is a prototypic member of a distinct family of G protein–coupled receptors that differs in structure from the other families comprising the superfamily of G protein–coupled receptors that are predicted to span cell membranes seven times (7, 10). This family of proteins includes the receptors for parathyroid hormone/parathyroid hormone–related peptide (12), secretin (13), vasoactive intestinal peptide (14), glucagon (15), glucagon-like peptide-1 (16), growth hormone releasing hormone (17, 18), pituitary adenylate cyclase–activating polypeptide (19), corticotrophin-releasing-factor (CRF) (20), gastric inhibitory polypeptide (21), and an insect diuretic hormone (22). CTRs (23, 24) and several related receptors (19, 25) activate both cAMP and accumulation of cytoplasmic Ca^{2+} second messenger pathways when transfected into receptor-negative cells. The structural mechanisms by which the CTR couples to the G proteins involved in these signaling pathways are yet to be elucidated in view of the unique amino acid sequences contained in the intracellular face of the CTR.

Comparison of the porcine renal CTR (10) to the human ovarian CTR (o-hCTR) (7) revealed the presence of a predicted nonhomologous 16-amino acid peptide insert in the first intracellular domain of the o-hCTR and suggested the existence of transcript splice variants and a complex gene structure, which was recently confirmed by the characterization of the porcine

Address correspondence to Alan H. Gorn, M.D., Arthritis Research, 149 The Navy Yard, 13th Street, Massachusetts General Hospital-East, Charlestown, MA 02129. Phone: 617-726-3742; FAX: 617-726-5651. J.-T. Wang's current address is Department of Dentistry, National Taiwan University Hospital, No. 1 Chang-Te Rd., Taipei, Taiwan, Republic of China.

Received for publication 5 October 1994 and in revised form 2 December 1994.

J. Clin. Invest.

0021-9738/95/06/2680/12 $2.00
Volume 95, June 1995, 2680–2691

1. *Abbreviations used in this paper:* CRF, corticotropin-releasing-factor; CT, calcitonin; CTR, CT receptor; EC_{50}, 50% maximum effective concentration; GC-2, a CTR isoform from GCT; GC-10, a CTR isoform from GCT; GCT, human giant cell tumor of bone; o-hCTR, a CTR isoform from human ovarian tumor cells (BIN-67); ORF, open reading frame; RF, restriction fragment; sCT, salmon CT; UTR, untranslated region.

CTR gene (26). The existence of splice variants is analogous to those of the dopamine D2 (27), growth hormone releasing hormone (17, 18), pituitary adenylate cyclase–activating polypeptide (19), CRF (20), or metabotropic glutamate (28) receptors. Such variants have not been described for most of the G protein–coupled receptors. The cloning of mouse and rat brain CTR cDNAs identified another receptor form that contained a predicted nonhomologous 37–amino acid insert in the second extracellular domain, as well as a form homologous to the original porcine kidney cell receptor (11, 29, 30). Different binding affinities were noted for these two rodent receptor forms (29, 30). These observations have confirmed the existence of multiple CTR forms (isoforms) in a single species. Isoforms of the CTR in bone, however, have not been characterized at the molecular level.

Osteoclasts (the bone cell type that expresses the CTR) have been partially purified in small quantities from bone tissues from several species but have not been maintained in culture (31). Although attempts have been made to isolate osteoclasts from human fetal bone (32), human fetal tissues are not readily available, and the viability of the isolated cells is poor. To overcome this problem, we chose to characterize potential human skeletal CTR variant(s) in the abundant osteoclast-like cells that are characteristic of human giant cell tumors of bone (GCT), an osteolytic neoplasm (33). Microscopically, GCTs are characterized by numerous osteoclast-like multinucleated giant cells interspersed among stromal cells. Although these tumors are heterogeneous, there is evidence that a population of stromal cells are the proliferating cells and, therefore, these cells have been considered to constitute the neoplastic population of the tumor (33–36). The multinucleated giant cells, on the other hand, are differentiated cells that rarely persist in culture and do not appear in lesions introduced into immunosuppressed mice (35, 37). These giant cells have been shown to fulfill current criteria for the characterization of in osso osteoclasts (38), including multinucleation, responsiveness to CT and expression of CTRs, the capacity to form resorption pits in devitalized bone, calcium-sensing, and the presence of tartrate-resistant acid phosphatase. These osteoclast-like cells, therefore, provide an abundant source of CTR mRNA (7) for molecular cloning.

We now describe the cloning and characterization of cDNAs from GCT RNA that encode two distinct isoforms of the human CTR. The first form (represented by a clone designated GC-10) differs from the o-hCTR (7) in the 5′-region in that it lacks a 71-bp segment that contains the first (more 5′-) of two in-frame AUG codons found in the o-hCTR, but retains the still more 5′-untranslated nucleotides. GC-10 is virtually identical to the o-hCTR clone in the more 3′-regions of the open reading frame (ORF), including the sequence encoding the putative first intracellular domain. Analysis of this new clone demonstrates that the most 5′-potential initiation codon found in the o-hCTR cDNA clone could be spliced in or out to create transcript variants that both encode functional CTRs when expressed in COS cells but may differ by 18 amino acids at the NH_2 terminus. The second human GCT-CTR cDNA variant (GC-2) lacks this 71-bp 5′-insert, but also lacks 48 nucleotides that encode part of the putative first intracellular domain. The two GCT-CTR isoforms, therefore, differ from each other only by the presence or absence of this 48-bp insert encoding part of the first intracellular domain. The ligand binding and cAMP responses of the expressed GCT-CTR isoforms differ markedly, however. The first intracellular loop of the CTR must therefore be an important modulator of these functions since the GCT-CTR isoforms differ only in this domain. Using in situ hybridization we also show that the CTR mRNA is expressed in GCT tissue osteoclast-like cells and we have mapped the human CTR gene to chromosome 7 in band q22.

Methods

Primary tissue and cultured cells. Specimens of human giant cell tumors of bone were obtained from Dr. H. J. Mankin (Massachusetts General Hospital, Boston, MA) at the time of tumor resection. Confirmation of histopathological diagnosis was obtained on all tumors. COS-M6 cells, subcloned from COS-M7 cells, were originally obtained from Dr. Brian Seed (Massachusetts General Hospital).

Isolation of human GCT-CTR cDNAs. Polyadenylated (poly[A]$^+$) RNA was prepared (39) from a primary GCT, and an aliquot of this RNA was shipped to Dr. B. Zurler (Miles Laboratory, West Haven, CT) for the preparation of a λ gt 23 cDNA library. We screened this library by plaque hybridization using a ^{32}P-labeled BglII-PstI restriction fragment probe from the o-hCTR cDNA (7). Hybridization was performed at 42°C in 40% formamide, and the filters were washed in 0.25 × SSC at 60°C. Isolated cDNAs were subcloned from the λ gt 23 phage vector into Bluescript SK(+) II plasmid vector (Stratagene, La Jolla, CA) for sequencing.

For isolation and analysis of PCR cDNA products, additional poly[A]$^+$ RNA was prepared, as before, from GCT tissue from two additional patients. First strand cDNA was synthesized from RNA from each patient using the cDNA Cycle Kit (Invitrogen, San Diego, CA). PCR primers were selected from the o-hCTR and cloned GCT-CTR sequences so that the predicted PCR products would include 5′-untranslated sequences (5′-to the first in-frame AUG of the o-hCTR) and the region encoding the first intracellular and second extracellular domains. These amplified regions would include, if present, the predicted sequence inserts contained in either the human ovarian or the rodent CTRs relative to the original porcine CTR clone. The PCR products derived from these primers also overlap the GCT-CTR 3′-fragment clones isolated from the cDNA phage library. The primer sequences (designated F1 and R2) are as follows: F1: [5′-CCTTTGCTTCTATTGAGCTGTG-3′], R2: [5′-CTGGTAATAGCATGGATAGTG-3′]. PCR reactions were set up using dedicated pipettes and barrier pipette tips (Molecular Bio-Products, San Diego, CA) in a laminar flow hood. All PCR runs included negative control reactions consisting of primers without template and template without primers. Before the reverse transcriptase reaction, the GCT poly[A]$^+$ RNA was subjected to RNAse-free DNAse (Boehringer-Mannheim Biochemicals, Indianapolis, IN) digestion (40) to remove any remaining genomic DNA and to further reduce the possibility of contamination from isolated cDNAs. PCR conditions were 2 min at 94°C ("hot start") before adding 2.5 U of *Taq* DNA polymerase (Promega Corp., Madison, WI) followed by 30 cycles of 94°C for 30 s; 55°C for 1 min; 72°C for 1 min, 30 s; ending with 10 min at 72°C. PCR reaction products were analyzed by agarose gel electrophoresis and ethidium bromide staining of 10% of the reaction volume followed by Southern blot analysis (39) using o-hCTR probes. PCR products were initially cloned using the pCR II vector (Invitrogen).

Sequencing and analysis of GCT cDNAs. Double-stranded template sequencing of both strands was performed on cDNAs subcloned into plasmids using the dideoxy nucleotide chain termination method (Sequenase kit; United States Biochemical Corp., Cleveland, OH) after alkaline or heat denaturation. Sequencing of bulk PCR reaction products was performed by the method of Kretz et al. (41) after isolating the appropriate band by electrophoresis in 1% Nusieve GTG agarose (FMC Corp. BioProducts, Rockland, ME). Both strands of the GCT cDNA phage library clone 6A were sequenced in entirety. The other four phage library–derived clones were sequenced at their 5′- and 3′-ends (except clone 1A) and over portions of their putative intra- or extracellular domains to assess the presence of variations in these clones that might

represent isoforms of the CTR. 10 PCR clones were also sequenced to assess variations that might represent receptor isoforms or mutations and to identify possible single nucleotide substitutions in a particular clone secondary to infidelities resulting from *Taq* DNA polymerase activity. Sequences were analyzed using the computer programs in Version 7 of the University of Wisconsin Genetics Computer Group (UWGCG) (42) and TopPred II (43).

Construction of full-length CTR cDNAs for expression studies. Full-length CTR cDNAs incorporating the unique regions found in the GCT-CTR cDNAs were prepared using the cloned GCT PCR products after sequencing 10 clones to confirm the fidelity of the selected clones. The selected clones were digested with EcoRI to isolate a restriction fragment (RF) that included the regions coding for the predicted alternative isoforms recognized among these clones. These EcoRI RFs begin at 5′-untranslated sequence (bp 143 of the o-hCTR) lying upstream of the first in-frame AUG in the o-hCTR and extend to nucleotides that encode the putative second intracellular domain (bp 875 of the o-hCTR). These RFs do not include any sequences from the PCR primers. The isolated GCT-CTR EcoRI-digested RFs were then ligated to the 3′-sequences of the o-hCTR cDNA contained in the pcDNA I expression vector (Invitrogen) to create sequences corresponding to the entire coding region of the GCT-CTR cDNAs. The regions of the o-hCTR used to create these constructs are identical to the GCT-CTR cDNAs isolated from the phage library with the exception of a single nucleotide substitution (C to T) corresponding to bp 1635 of the o-hCTR sequence. The 3′-o-hCTR sequences were prepared for subcloning by excision of the corresponding o-hCTR EcoRI fragment and deletion of a major section of the 3′-untranslated region (3′-UTR) 3′-to the NsiI site. In these constructs, therefore, potential 3′-RNA degradation signals are deleted. We reasoned that deletion of these 3′-UTR sequences and the resulting smaller plasmid construct might permit higher levels of CTR expression after transfection. An o-hCTR construct with the 3′-UTR NsiI RF deletion was prepared in the same manner. The orientation and fidelity of ligation products were verified by RF digestion and nucleotide sequencing of the completed constructs. The two different GCT-CTR constructs, designated GC-2 and GC-10, represent native GCT-CTR cDNAs with full-length ORFs determined from the isolated overlapping clones from which they were constructed. They differ from the cloned o-hCTR isoform encoding cDNA as described in Results and in Fig. 2.

Transfection of COS-M6 cells with CTR cDNAs. "Maxi-prep" plasmid DNA prepared using QIAGEN tips (QIAGEN, Inc., Chatsworth, CA) was used to transfect COS-M6 cells grown in 10-cm plastic dishes (Falcon Plastics, Lincoln Park, NJ) using a DEAE-Dextran/chloroquine procedure (44). Transfection efficiency was determined for each plasmid-CTR isoform construct preparation on a fraction of the transfected cells after plating them on 3-cm plastic dishes and performing in situ ^{125}I-salmon (s) CT binding followed by fixation, counter staining with methylene blue, and emulsion autoradiography using NTB-2 photoemulsion (Eastman Kodak Co., Rochester, NY) (35). The percentage of COS cells expressing receptors, indicated by the heavy accumulation of silver grains, was quantitated by counting multiple fields under a magnification of 100 for a total count of at least 1,000 cells per transfection.

cAMP assay and radiolabeled CT binding in COS-M6 cells transfected with CTR-cDNAs. Radioligand binding and cAMP assays were performed in triplicate 48 h after transfection, as previously described (7). To correlate receptor binding with levels of ligand-induced cellular cAMP, ligand binding and cAMP measurements were performed in parallel on cells transfected in the same 10-cm culture dishes after splitting and replating. A fraction of the transfected cells used in these assays was also plated on 3-cm plastic dishes to determine the transfection efficiency of each plasmid/CTR cDNA. This protocol permitted the quantitation of CTR-expressing cells in each experiment and the number of receptors expressed per transfected cell using Scatchard analysis.

Analysis of CTR mRNA expression in GCT by in situ hybridization. Frozen unfixed sections (8–10 μm) from five separate GCT tissues were thaw-mounted on gelatin-coated, RNAse-free slides after sectioning on a cryostat at −18°C. Before prehybridization, slides were fixed in 4% paraformaldehyde and treated with 0.2 N HCl, proteinase K, 0.25% acetic anhydride, 2 × SSC followed by dehydration and delipidation. Templates for in vitro transcription of riboprobes for the human CTRs were prepared by subcloning a 642-bp EcoRI/ApaI RF from the o-hCTR cDNA into the vector Bluescript SK II (Stratagene). ^{35}S-labeled sense and antisense riboprobes were then prepared using T3 or T7 polymerase to transcribe the linearized plasmid DNA using the Riboprobe System (Promega Corp.). After hybridization at 55°C in 50% formamide, autoradiography was carried out by dipping the slides in Kodak NTB-2 emulsion, followed by air drying at room temperature and exposure at 4°C.

Mapping the human CTR gene by in situ hybridization to metaphase chromosomes coupled with selective PCR amplification using DNA from somatic hybrid cells. The ~ 3.6-kb o-hCTR cDNA in pcDNA I (Invitrogen) was cesium-purified and labeled by nick translation to a specific activity of 1.3×10^7 cpm/μg with [^{3}H]dATP, [^{3}H]dCTP, [^{3}H]-dGTP, and [^{3}H]dTTP (DuPont/New England Nuclear, Boston, MA), as previously described (45). Human metaphase chromosomes were prepared from cultures of peripheral blood lymphocytes from two normal males. In situ hybridization was performed with minor modification of the method previously reported (45). Hybridized slides were coated with Kodak NTB-2 emulsion and stored in a desiccator at 4°C for 21 d. After development of the autoradiographs, chromosomes were stained in a 50 μg/ml solution of quinacrine mustard dihydrochloride. Locations of silver grains were recorded with reference to an idiogram of G-banded metaphase chromosomes at the 400 band stage.

To confirm and clarify the CTR gene location results obtained by in situ hybridization, DNA from human-hamster somatic cell hybrids (NA10629 and NA10791 from the NIGMS Human Genetic Mutant Cell Repository, Camden, NJ) that contained selected chromosomes was analyzed by PCR under species-specific conditions. Human-specific CTR primers corresponding to regions homologous to exons identified in the mouse CTR gene (11) were synthesized and paired to allow PCR amplification of two exons and an intervening intron. The primer pair E1-F [5′-CTTCCTGCCTTTTCAAATCAAACC-3′] and E2-R [5′-TCCGGAAAATAATCTGGGCAGAAC-3′] was used (500 ng of each primer) along with 100 ng of DNA from human-hamster (Chinese hamster ovary cell) somatic cell hybrids or total human or hamster DNA as template in 100-μl reaction volumes. Cycling conditions were: 6 min at 94°C ("hot start"); 45 s at 94°C; 1 min at 55°C; 3 min at 72°C for 30 cycles, then 10 min at 72°C. *Taq* DNA polymerase, 2.5 U (Promega Corp.), was added after the hot start; the optimized Mg concentration was 2.0 mM. PCR amplification products (10–30% of reactions) were analyzed by agarose gel electrophoresis and Southern blot analysis (39) using a ^{32}P-labeled BglII-PstI RF probe from the o-hCTR. To confirm the specific PCR amplification of the human CTR gene, the positively hybridizing single band amplified from the somatic cell hybrid containing chromosome 7 was cloned into pCR II (Invitrogen) and sequenced.

Results

Cloning and sequence analysis of GCT-derived CTR cDNAs. Five independently isolated clones were obtained after screening ~ 3.6×10^6 plaques from a GCT-cDNA library using plaque hybridization. Insert size ranged from ~ 2.5 to 2.8 kb. Although these clones differed in length at their 3′-ends, they began at exactly the same 5′-end corresponding to nucleotide 1051 of the previously reported o-hCTR sequence (7) which encodes part of the putative third transmembrane domain (Fig. 1). No positively hybridizing plaques were identified when ~ 1.2×10^6 additional plaques were screened with a cDNA probe from the 5′-region of the o-hCTR. The ORFs of the isolated clones were identical to the o-hCTR clone except at the nucleotide corresponding to position 1635 of the o-hCTR

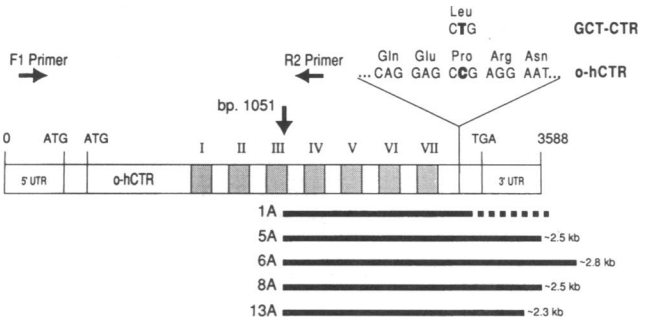

Figure 1. Localization of the five clones isolated from the GCT-CTR cDNA phage library relative to the o-hCTR cDNA sequence. Stippled areas of the o-hCTR bar diagram indicate nucleotides predicted to encode transmembrane domains I to VII (not to scale). Note the position of the two in-frame ATG (AUG) initiation codons in the o-hCTR. The truncated GCT-CTR cDNA clones (designated *1A, 5A, 6A, 8A,* and *13A*) are depicted as line diagrams. All five GCT-derived clones begin at the same 5′-position corresponding to bp 1051 of the o-hCTR sequence. The interrupted line at the 3′-end of clone 1A indicates that this clone was not sequenced at its 3′-end. The ORF of the GCT-CTR clones differed from that of the o-hCTR only by a single base (C to T) substitution corresponding to bp 1635 of the o-hCTR cDNA. This change would result in the substitution of a Leu for a Pro in the putative COOH-terminal intracellular region of GCT receptor proteins. The positions of the PCR primers (*F1* and *R2*) used to generate the 5′-portion of the GCT-CTR cDNAs are indicated by horizontal arrows.

sequence where a C in the o-hCTR sequence was replaced by a T in all five of the GCT cDNA clones (Fig. 1). This nucleotide change would result in the substitution of a leucine for a proline at the residue corresponding to 463 in the COOH-terminal intracellular region of the predicted o-hCTR protein sequence. Resequencing of the o-hCTR clone over this region confirmed the reported sequence and demonstrated that this difference is not the result of a sequencing error. This point mutation may represent a polymorphism among RNAs from different sources, although other possibilities such as a cloning artifact or a somatic cell mutation in the cultured BIN-67 ovarian tumor cells, from which the o-hCTR cDNA was isolated, cannot be ruled out. Truncation of all five clones at the same 5′-position may have resulted from events associated with construction or amplification of the cDNA library such as the presence of secondary RNA structures that inhibited reverse transcription or of sequences or secondary structures that prevented representational amplification of complete CTR-encoding clones during amplification of the library.

Reverse transcription-PCR was used to characterize the remaining 5′-sequence of GCT-CTR cDNAs. Specific primers were based on the known sequences from the GCT and o-hCTR clones and were designed to produce products that would include regions of overlap with the existing GCT-CTR cDNAs so that full-length cDNAs could be generated (Fig. 1). The primers F1 and R2 yielded a major band of the predicted size (1035 bp). Subtle differences in size among possible multiple products running together in this large single band would not be resolved by this method (e.g., a 48-bp difference out of 1035 bp). Southern blot hybridization of the PCR reaction products after agarose gel electrophoresis using a ^{32}P-labeled o-hCTR probe did not demonstrate the presence of any minor bands sufficiently different in size to be resolved from the strongly hybridizing single band produced by this reaction.

The product generated by the F1/R2 primer set was separated by electrophoresis in low temperature melting agarose and directly sequenced using overlapping inside primers from the regions that encode the predicted first intracellular and second extracellular domains. This method of bulk PCR product sequencing was used to establish the sequence of the major (mathematically most abundant) CTR sequence contained in the isolated band. Rare or less abundant sequence variants (or potential point mutations representing *Taq* DNA polymerase infidelities) that would comigrate with the major product would not be detected by this method, however. DNA from the same isolated PCR product band was, therefore, also cloned into pCR II. 10 PCR-product clones were isolated and sequenced to characterize less abundant GCT-CTR isoform variants over this region and rule out inconsistent point mutations resulting from *Taq* DNA polymerase infidelities in clones selected for use in further constructions.

Bulk sequencing of the PCR product revealed that the major GCT-CTR isoform (GC-2 in Fig. 2) does not contain the 48-bp insert found in the o-hCTR corresponding to the region predicted to encode the first intracellular domain. This major product (and by extrapolation, the major transcript) also does not contain the 111-bp insert encoding for 37 additional amino acids in the second extracellular domain of the mouse and one rat (C1b) brain CTR isoform (11, 29, 30). Sequencing of the 10 cloned PCR products revealed that 7 of the 10 clones (represented by clone GC-2) did not contain the 48-bp insert, confirming that this cDNA represents the most abundant transcript derived from GCT mRNA. These seven (GC-2) clones also differed from the o-hCTR in the 5′-region in that none possessed an insert of 71 bp that included the most 5′-in-frame start site found in the o-hCTR. As previously noted (7), both the 5′- and 3′-AUG codons found in the o-hCTR clone have an A at the minus 3 position consistent with and sufficient for the minimal Kosak consensus start site (46). The remaining 3 of the 10 sequenced clones (represented by clone GC-10) also differed from the o-hCTR cDNA in that none contained the 71-bp 5′-insert of the o-hCTR. The GC-2 and GC-10 nucleotide sequences immediately 5′- and 3′-to the point where the 71-bp insert is located in the o-hCTR cDNA were identical to the o-hCTR sequence with the exception of a single base in the minus 6 position relative to the more 3′-AUG of the o-hCTR (Fig. 2 *B*). The GC-2 and GC-10 clones, therefore, both possess only a single in-frame AUG homologous to the second (3′-) in-frame AUG found in the o-hCTR. The GCT clones represented by GC-10 did, however, possess the other insert of 48 bp found in the o-hCTR (but not in GC-2) in the region encoding the predicted first intracellular domain. This 48-bp insert would be spliced in between a codon of the GC-2 cDNA, resulting in the sequence AGG instead of AGA. Since both of these triplets encode an arginine residue, the predicted amino acid sequence of GC-2 is conserved adjacent to the inserted peptide in the GC-10 and o-hCTR isoforms (Fig. 2 *C*). We have confirmed the presence of both GC-2 and GC-10 isoforms in the GCT RNA from each of the two patients tested.

In summary, the isoform encoded by GC-10 is identical to the o-hCTR except that its NH_2-terminal sequence lacks 18 predicted amino acids due to the absence of a 5′-in-frame initiation codon and other inserted nucleotide sequences found in the o-hCTR cDNA. The predicted receptor isoform encoded by GC-2 also lacks these NH_2-terminal 18 amino acids and, in addition, lacks the sequence of 16 amino acids found in the

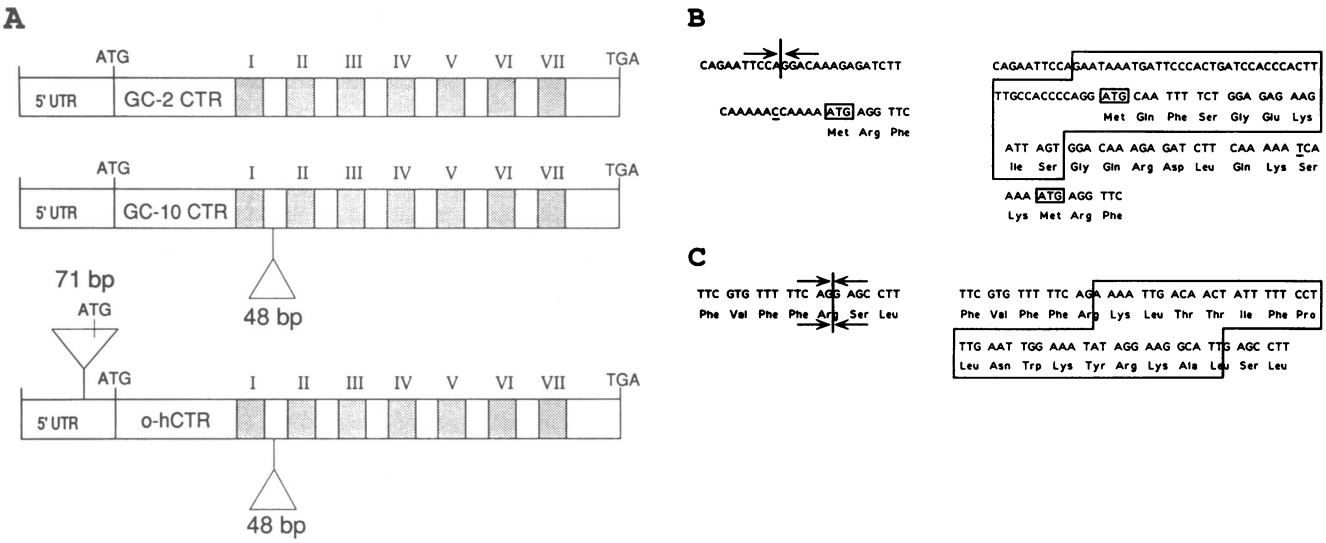

Figure 2. Comparison of sequence differences between the two GCT-CTR cDNA clones (GC-2 and GC-10) and the o-hCTR cDNA. (*A*) Bar diagrams representing the GC-2, GC-10, and o-hCTR cDNAs. Stippled regions indicate sequences encoding the putative transmembrane domains of each receptor. The 5′-region of the o-hCTR cDNA includes a 71-bp insert containing an additional in-frame initiation codon not present in the two GCT-CTR cDNAs. Both GC-10 and o-hCTR contain a 48-bp insert relative to GC-2 that encodes 16 additional amino acids in the putative first intracellular domain. (*B*) Nucleotide and predicted amino acid sequence in the region of the 5′-insert of 71 bp present in the o-hCTR cDNA. Potential in-frame initiation codons are boxed. The sequence from the two GCT cDNAs (GC-10 and GC-2) is shown on the left. The arrows and break line indicate the putative splice point where the 71-bp sequence is inserted in the o-hCTR cDNA. This 71-bp sequence is outlined in the o-hCTR sequence at the right. This insert encodes 18 amino acids not found in the GCT-CTR cDNAs. A single base substitution (T to C) present at the -6 position in the GCT-CTR cDNAs compared with the o-hCTR sequence is indicated by underlining. (*C*) Nucleotide and predicted amino acid sequence in the region of the putative first intracellular domains of the three CTR clones. GC-2 sequence is on the left with the arrows and break line indicating the putative splice point where the 48-bp sequence is inserted in the GC-10 and o-hCTR cDNAs. This 48-bp insert is outlined in the sequence on the right and encodes an additional 16 amino acids in the putative first intracellular domains of the GC-10 and o-hCTR isoforms not present in GC-2.

putative first intracellular domains of the o-hCTR and GC-10 clones. GC-2 is, therefore, homologous to the porcine renal receptor (10) in the putative NH_2-terminal region and in the first intracellular domain.

Characterization of ^{125}I-CT binding to COS-M6 cells transfected with o-hCTR, GC-2, and GC -10 CTR cDNAs. COS-M6 cells were transfected with each of the three distinct human CTR cDNAs representing the three isoforms, as described above. In each of these constructs, part of the 3′-UTR 3′-to the NsiI restriction site was deleted to increase expression. All three constructs are, therefore, identical over the region 3′-to the 48-bp insert contained in the o-hCTR and GC-10 clones. Binding of ^{125}I-sCT was assayed in triplicate for each encoded isoform in parallel with the other two isoforms in the same assay so that differences could be directly ascertained. Transfection efficiencies were obtained for each isoform construct using in situ ^{125}I-sCT binding and emulsion autoradiography to quantitate the percentage of receptor-expressing cells.

Scatchard analysis of CT binding for each of the three receptors was consistent with the presence of a single class of high affinity CT-binding sites. Transfection efficiency was 9.2% for the o-hCTR, 10.6% for GC-10, and 14.4% for GC-2. The receptor number per transfected cell ranged from $\sim 2 \times 10^6$ to $\sim 3 \times 10^7$. Transfection with cDNA preparations of GC-2 consistently resulted in a higher level of receptor expression than with GC-10 or o-hCTR cDNAs. The apparent K_d for sCT in COS cells transfected with either the o-hCTR or GC-10 cDNAs was similar. The mean K_d for the o-hCTR was $\sim$ 1.4 nM (range 0.44–3.8 nM in four experiments) compared with $\sim$ 1.6 nM for GC-10 (range 0.61–2.9 nM in four experiments). The mean K_d for sCT for GC-2–transfected COS cells was $\sim$ 15.0 nM (range 10.7–21.2 nM in four experiments), or $\sim$ 10 times higher than the K_d for the o-hCTR or GC-10 isoforms. Parallel binding curves (Fig. 3) for ^{125}I-sCT competed with unlabeled sCT in COS cells transfected with each isoform-encoding cDNA confirmed the relative lower affinity of the GC-2 isoform (corresponding to its higher K_d by Scatchard analysis) compared with the o-hCTR and GC-10 isoforms (Fig. 3). The range of K_d values for sCT for the o-hCTR in these experiments was similar to those previously calculated for the o-hCTR (range 0.44–2.1 nM [7]), confirming that the partial deletion of the 3′-UTR in the constructs used in these experiments did not affect binding affinity.

Characterization of CT-induced cAMP responses in COS-M6 cells transfected with the o-hCTR, GC-2, and GC-10 cDNAs. Incubation with CT elicited a concentration-dependent increase in cAMP levels in COS cells transfected with all three CTR isoform-encoding cDNAs (Fig. 4). Maximum stimulatory concentrations of CT resulted in cAMP levels that differed for each of the three isoforms (Figs. 4 and 5). Transfection of the GC-2 isoform and incubation of the cells with sCT resulted in the greatest maximal cAMP level with a mean of $\sim$ 28.7-fold over control per 2×10^4 transfected cells (range 25.4- to 32.0-fold in three experiments) (Fig. 5 *A*). The mean maximal cAMP level after incubation with sCT for GC-10 was 3.3-fold over control per 2×10^4 transfected cells (range 2.6- to 4.3-fold in three experiments) (Fig. 5 *A*) and $\sim$ 2.4-fold over control per 2×10^4 transfected cells (range 2.1- to 2.6-fold in two experi-

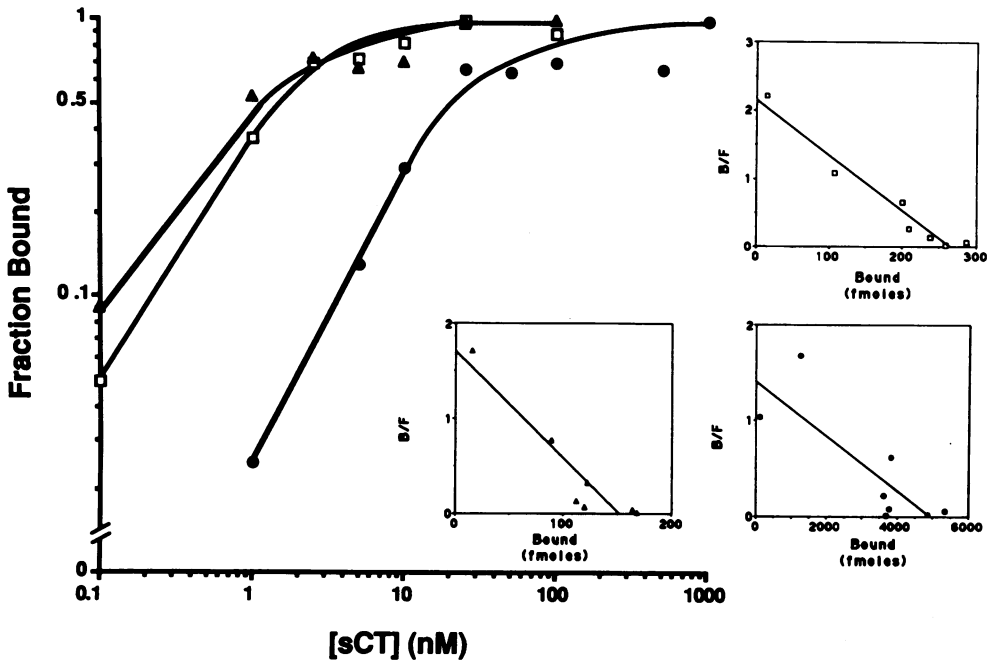

Figure 3. Salmon CT binding to COS cells transfected with the o-hCTR (*filled triangles*), GC-10 (*open boxes*), and GC-2 (*filled circles*) CTR isoform-encoding cDNAs. Transfected COS cells were incubated with ~ 6 fM of radioiodinated salmon CT (2,422 Ci/mmol) in the presence of increasing amounts of unlabeled ligand for ~ 18 h at 4°C. Data points represent the means of triplicate measurements. Maximal binding per tube averaged 10,576 cpm for the o-hCTR; 13,781 cpm for GC-2; and 11,260 cpm for GC-10. Binding per tube in the presence of 10 μM unlabeled salmon CT averaged 402 cpm for o-hCTR; 654 cpm for GC-2; and 448 cpm for GC-10. There was no significant CT binding to mock-transfected COS cells (10). The mean K_d for each receptor isoform was determined from the K_d values calculated by Scatchard analysis(*insets*) in four separate experiments. The K_d for o-hCTR was 1.41 nM (range 0.44–3.77 nM); for GC-10 the K_d was 1.57 nM (range 0.61–2.91 nM); and for GC-2 the K_d was 14.96 nM (range 10.70–21.23 nM).

ments) for o-hCTR (not shown). Maximal cAMP responses for each receptor-encoding cDNA were assayed in parallel experiments. The marked difference in maximal cAMP stimulation between GC-2 and GC-10 was still apparent when the cAMP response was normalized to receptor number (Fig. 5 *B*). Cells transfected with the GC-2 receptor and incubated with sCT increased cAMP content to a mean maximum of 23.5 pmol/receptor $\times$ 10^{-10} (range 17.7–31.7 pmol/receptor $\times$ 10^{-10}) compared with 8.0 pmol/receptor $\times$ 10^{-10} (range 6.0–9.7 pmol/receptor $\times$ 10^{-10}) for the GC-10 receptor. Transfection with the GC-2 or GC-10 cDNAs resulted in the expression of a high number of receptors in the COS cells ($\geq 2.1 \times 10^6$ receptors/cell). The level of expression for each receptor was above the threshold value for absolute maximal cAMP stimulation, based on the results observed for the individual CTR receptor isoforms (i.e., at these levels of receptor expression, cAMP accumulation after incubation with the appropriate ligand concentration was maximal [or saturated] and did not increase further as the receptor number per cell increased). These data suggest that the observed difference in ligand-induced increase in cAMP content between GC-2 and GC-10 is the result of the difference in predicted receptor structure involving the first intracellular domain and is not the result of differences in receptor expression. This difference in structure of the CTR must therefore influence the coupling of each receptor isoform to the G protein/adenylate cyclase system in COS cells.

The magnitude of the maximal cAMP response produced by salmon or human CT is approximately the same for any given receptor isoform expressed in COS cells (Fig. 4, *B* and *C*). The EC_{50} values for salmon and human CTs, however, reflect the greater potency of sCT (Fig. 4, *B* and *C*). The EC_{50} value for sCT is ~ 0.2 nM for GC-2 and ~ 6 nM for GC-10. The magnitude of the cAMP response of the GC-2 isoform is increased despite its lower ligand binding affinity (higher K_d) compared with the GC-10 and o-hCTR isoforms and appears to reflect a greater efficiency in coupling of the ligand-occupied GC-2 CTR to cAMP production. The GC-2 isoform is, therefore, capable of signaling through cAMP at concentrations of ligand that do not elicit increases in cAMP levels in COS cells transfected with the GC-10 or o-hCTR isoforms.

Localization of CTR mRNA expression in GCTs by in situ hybridization. To determine which cells in GCTs express CTR mRNA, we analyzed sections from five tumors by in situ hybridization using sense and antisense o-hCTR riboprobes. We observed that expression of CTR mRNA is localized primarily to multinucleated giant cells and smaller multinucleated cells with characteristics of osteoclast-like cells (Fig. 6). A small number of mononucleated cells also expressed CTR mRNA. Some of these mononuclear cells could be found near or adjacent to the CTR-positive multinucleated cells. The CTR mRNA-expressing mononuclear cells constituted a small minority of the mononuclear cell component of the tumors and may represent a distinct subpopulation of cells dispersed among the numerous mononuclear stromal cells. The presence of these CTR-positive cells is consistent with current hypotheses that multinucleated osteoclasts are formed from a pool of specific mononuclear osteoclast precursors.

Chromosomal mapping of the human calcitonin receptor. In situ hybridization using the complete o-hCTR cDNA to probe spread metaphase chromosomes was performed. A total of 254 silver grains were found from an analysis of 193 metaphase spreads. 20 grains (7.9%) were localized on chromosome 7, and, of these, 8 (3.1% of the total and 40% of the chromosome 7 grains) were confined to 7q22. A schematic representation of chromosome 7 showing the location of the observed silver grains is depicted in Fig. 7. A secondary peak was observed on chromosome 6 with 5 silver grains located on or directly beside band p12.

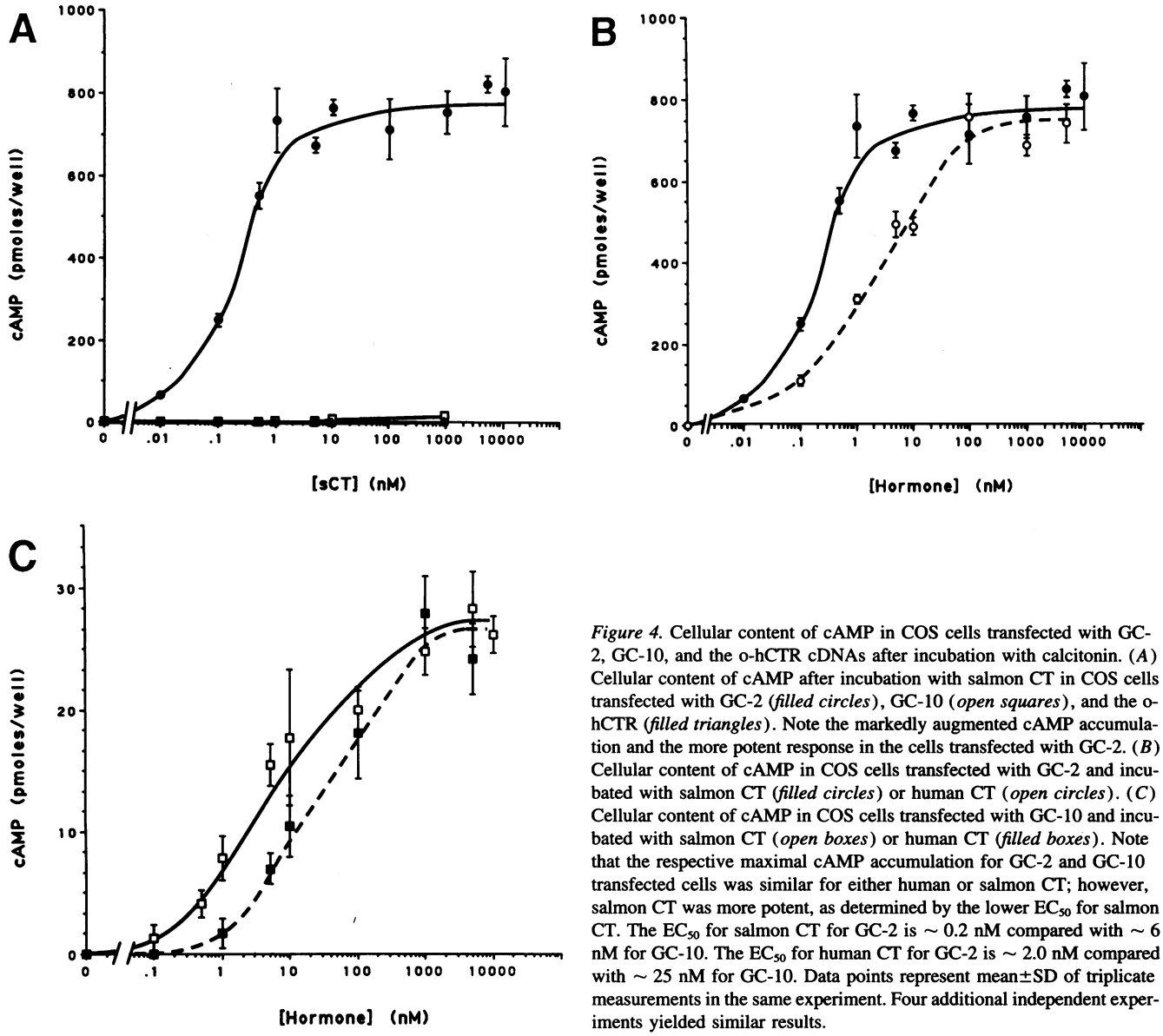

Figure 4. Cellular content of cAMP in COS cells transfected with GC-2, GC-10, and the o-hCTR cDNAs after incubation with calcitonin. (*A*) Cellular content of cAMP after incubation with salmon CT in COS cells transfected with GC-2 (*filled circles*), GC-10 (*open squares*), and the o-hCTR (*filled triangles*). Note the markedly augmented cAMP accumulation and the more potent response in the cells transfected with GC-2. (*B*) Cellular content of cAMP in COS cells transfected with GC-2 and incubated with salmon CT (*filled circles*) or human CT (*open circles*). (*C*) Cellular content of cAMP in COS cells transfected with GC-10 and incubated with salmon CT (*open boxes*) or human CT (*filled boxes*). Note that the respective maximal cAMP accumulation for GC-2 and GC-10 transfected cells was similar for either human or salmon CT; however, salmon CT was more potent, as determined by the lower EC_{50} for salmon CT. The EC_{50} for salmon CT for GC-2 is ~ 0.2 nM compared with ~ 6 nM for GC-10. The EC_{50} for human CT for GC-2 is ~ 2.0 nM compared with ~ 25 nM for GC-10. Data points represent mean±SD of triplicate measurements in the same experiment. Four additional independent experiments yielded similar results.

To definitively confirm the chromosomal locus of the CTR gene, we attempted to amplify by PCR a portion of the human CTR gene from human-hamster somatic cell hybrids that contained either human chromosome 6 or 7. These reactions used PCR primers from human CTR cDNA sequences (Fig. 8) that corresponded to two exons identified in the mouse CTR gene (11). These primers were specific for human DNA samples and produced a single PCR product of ~ 2 kb when total human DNA was used as template (not shown). PCR reactions using these primers did not produce any product when total hamster DNA was used as template (Fig. 8 *A*). Ethidium bromide staining of the PCR products amplified from human-hamster somatic cell hybrid DNA after agarose gel electrophoresis (not shown) revealed that a band of the expected size was obtained only from the somatic cell hybrid DNA that contained chromosome 7. DNA from the hybrid that contained chromosome 6 did not yield a visible product. Southern blot analysis of this gel using a ^{32}P-labeled o-hCTR probe (Fig. 8 *A*) confirmed the identity of the band amplified from human chromosome 7 and did not detect any hybridizing bands amplified from chromosome 6 DNA. We cloned the ~ 2-kb PCR product amplified from the chromosome 7 containing hybrid cell DNA into the vector pCR II and sequenced it from both ends; the predicted human CTR exon sequences downstream of both of the selected PCR primers were found. These exon sequences flanked an intron that included appropriate splice junctions (Fig. 8 *B*). These results, taken together with those obtained by chromosomal analysis using in situ hybridization, indicate that the human CTR gene resides on chromosome 7 at band q22.

Discussion

We have characterized cDNAs encoding two skeletal tissue CTR isoforms derived from human GCT of bone and compared these GCT-CTRs with the human ovarian CTR that we cloned previously (7). The three receptor isoforms differ by the presence or absence of two inserted sequences. The first insert includes an upstream start site that encodes a putative additional

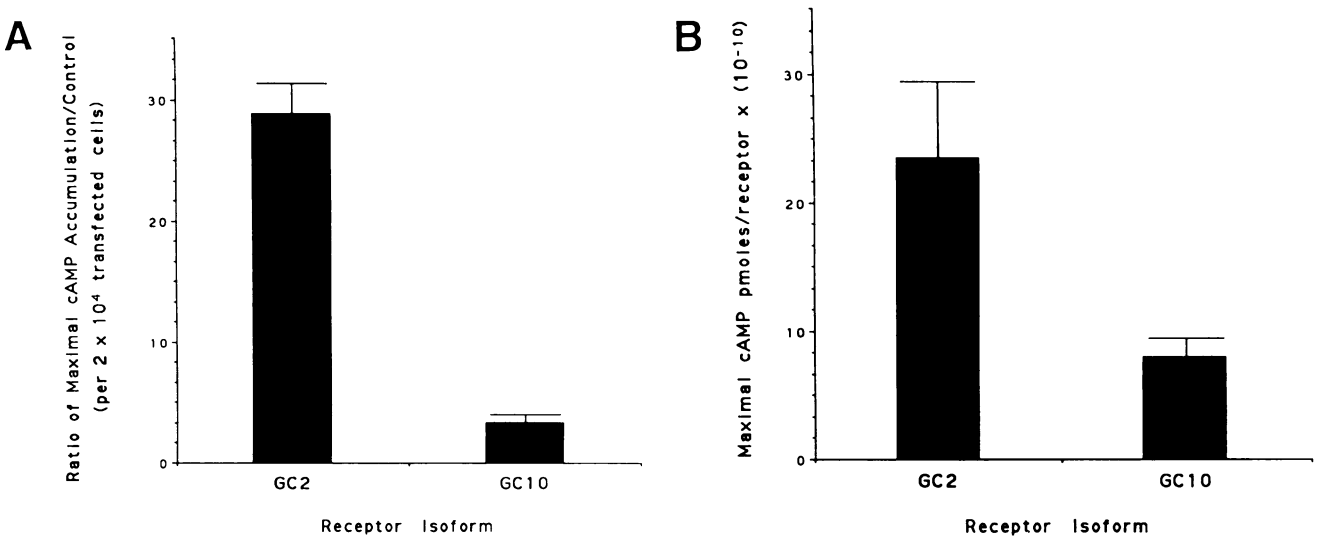

Figure 5. Comparisons of mean maximum cellular content of cAMP after incubation with salmon CT in COS cells transfected with GC-2 and GC-10 cDNAs. (*A*) Mean maximum cAMP accumulation/control per 2×10^4 transfected cells. The mean maximum cAMP accumulation per 2×10^4 transfected cells was 28.7-fold over control in cells transfected with GC-2 (range 25.4- to 32.0-fold in 3 separate experiments) compared with 3.3-fold over control in cells transfected with GC-10 (range 2.6- to 4.3-fold in 3 separate experiments). (*B*) Mean maximum cellular content of cAMP over control normalized for receptor number. The mean maximum content of cAMP in pmol/receptor ($\times 10^{-10}$) for cells transfected with GC-2 was 23.5 (range 17.7–31.7 in 3 separate experiments) compared with 8.0 for cells transfected with GC-10 (range 6.0–9.7 in 3 separate experiments). The maximum cAMP response was determined for each separate experiment by concentration-response curves that demonstrated saturation for each transfected CTR isoform-encoding cDNA. The data represent the mean±SD of the maximum cAMP response of transfected cells from three separate experiments in which ligand binding studies for Scatchard analysis were performed in parallel. Transfection efficiency was measured by in situ ^{125}I-salmon calcitonin binding and photoemulsion autoradiography on the transfected cells (see Methods).

18 amino acids at the NH_2-terminal end of the CTR or CTR proprotein in the o-hCTR isoform. This 5′-insert is absent in the GCT-CTR cDNAs. The second insert encodes an additional sequence of 16 amino acids in the putative first intracellular domain. This insert is present in the predicted first intracellular domain of one of the GCT-CTR isoforms (GC-10) and in the

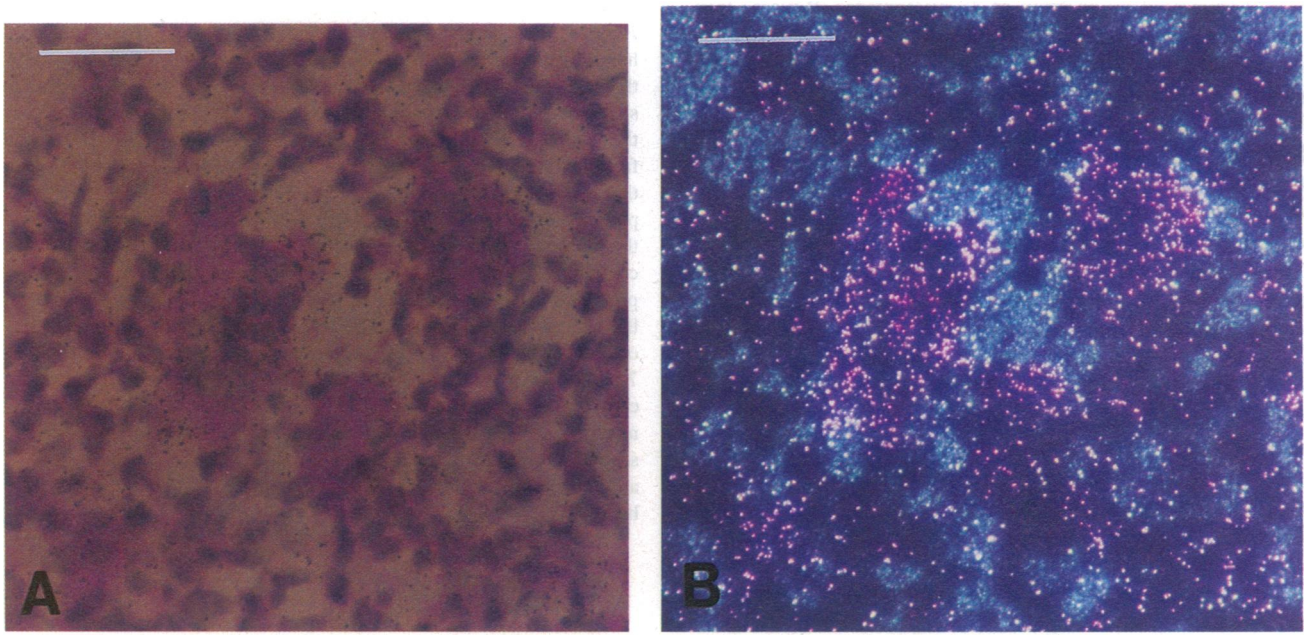

Figure 6. Localization of CTR mRNA expression by in situ hybridization and emulsion autoradiography in GCT tissue sections. A bright-field photomicrograph of a GCT section is shown in *A* and a dark-field photomicrograph of the same field is shown in *B*. Expression of CTR mRNA is indicated by the presence of silver grains primarily overlying multinucleated giant cells after hybridization to the ^{35}S-labeled antisense CTR riboprobe. A minority of mononuclear cells also appeared to hybridize to the CTR probe. These mononuclear cells may represent a distinct subpopulation of cells dispersed among the much more numerous mononuclear stromal cells that do not express CTR mRNA. There was no detectable hybridization in tissue sections using the sense riboprobe (data not shown). Scale bar, 50 μm.

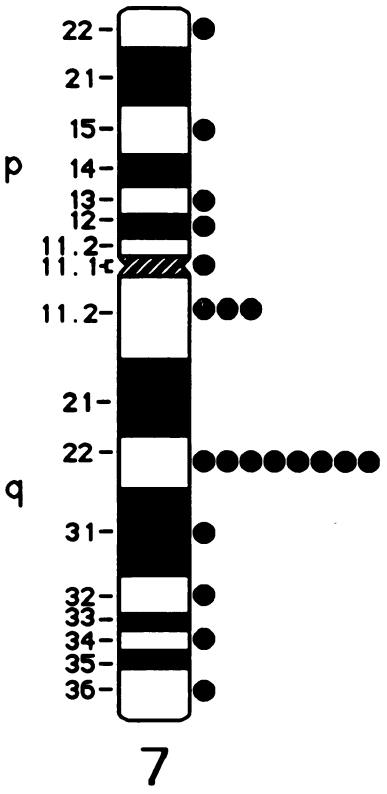

Figure 7. Idiogram of human chromosome 7 showing the location of silver grains after in situ hybridization of the human ovarian calcitonin receptor cDNA probe; a peak was seen at 7q22.

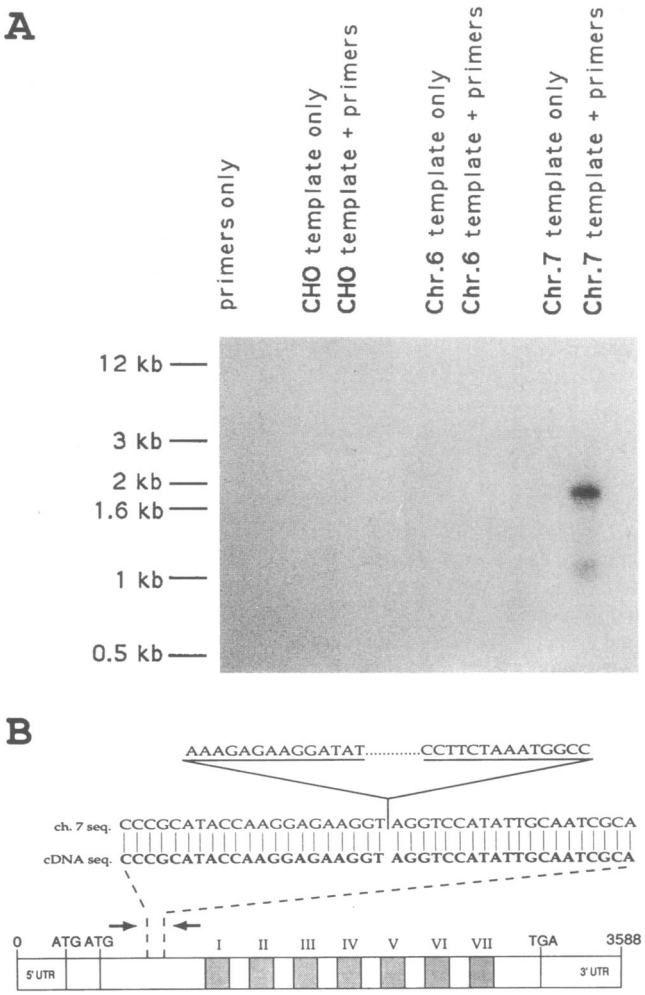

Figure 8. PCR amplification of the human CTR gene from human-hamster somatic cell hybrids. Human-hamster somatic cell hybrid DNA that contained either human chromosome 6 or chromosome 7 was chosen to verify the chromosome 7 location of the CTR gene indicated by the in situ hybridization results (see Results and Fig. 7). Primers derived from human CTR sequences corresponding to two exons identified in the mouse CTR gene were used. (*A*) Southern blot of PCR reaction products using an o-hCTR cDNA probe. This blot demonstrates that the human CTR primers are specific for human DNA from the hybrid containing chromosome 7 and not chromosome 6. The ~ 2-kb PCR product obtained is consistent with the presence of an intron between the two exon based primers. (*B*) Diagram showing partial sequence obtained from the ~ 2-kb PCR product amplified from the chromosome 7 containing hybrid. The location of the PCR primers in the o-hCTR cDNA is indicated by arrows. The PCR product sequence shown (designated *ch. 7 seq.*) includes parts of two exons interrupted by intron sequence (inserted at top). Taken together, the data shown in Figs. 7 and 8 demonstrate that the CTR gene is located on chromosome 7 at band q22.

o-hCTR isoform, but is absent in the second GCT isoform (GC-2).

The porcine CTR gene sequence recently characterized by Zolnierowicz et al. (26) revealed two potential splice sites in intron 7 separated by an exon of 48 nucleotides. Reverse transcription-PCR of porcine LLC-PK_1 cell RNA confirmed the presence of a low abundance transcript variant that included these 48 nucleotides (26). These findings indicate that porcine CTR variants are generated by alternative splicing of primary RNA transcripts. The encoded 16–amino acid insert in the first intracellular domain of the longer porcine variant contains only two residues identical to those in the 16–amino acid insert of the o-hCTR and GC-10 human sequences. The functional role of this insert in the porcine receptor was not determined by Zolnierowicz et al. (26). Localization of the human CTR gene to the -q arm of human chromosome 7, as described here, is consistent with our localization of the mouse CTR gene to the mouse chromosome 6 (11); mouse chromosome 6 is homologous to human chromosome 7. Although the porcine CTR has been localized to chromosome 9, the map of the porcine genome is incomplete and we cannot relate this localization to the human and mouse data. Our gene mapping indicates that the human CTR gene also contains introns (Fig. 8) and resides at a single location. These observations are consistent with the existence of only one human CTR gene and of alternative splicing of primary transcripts of this gene as the mechanism by which the human CTR isoforms are generated. Several other G protein–coupled receptor genes have been shown to encode multiple isoforms through alternative splicing (17–20, 27, 28), including a recently described CRF receptor variant that contains a predicted 29–amino acid insert of unknown function in the first intracellular domain (20).

Both of the GCT-CTR isoforms that we identified bind CT with high affinity; the GC-2 CTR isoform, however, has a lower binding affinity than the GC-10 isoform. Expression of the GC-2 receptor-encoding cDNA in COS cells produced a markedly augmented cAMP response after incubation with either salmon or human CT, compared with GC-10. The GC-2 receptor, despite its lower ligand binding affinity, demonstrated a lower

EC_{50} for CT as well as a greater maximal cAMP response. These data suggest that the GC-2 receptor is able to mediate cAMP-second messenger signaling over a broad range of ligand concentrations, including concentrations too low to induce cAMP accumulation by coupling to the GC-10 receptor isoform. The differences in second messenger coupling between the GC-2 and GC-10 receptor isoforms suggest a potential mechanism for adaptation to the different local ligand concentrations involved in paracrine or endocrine ligand-receptor interactions and may also explain certain pharmacological responses to CT. For example, a shift in the predominant CTR isoform could account for some of the variability in responses to calcitonin in patients with Paget's disease and other metabolic bone diseases.

Since the two GCT-CTR isoforms differ only in the first intracellular domain and were expressed in the same COS background, other structural determinants or differences in the expressed cell signal–coupling machinery cannot be evoked to explain the differing functional properties of these isoforms. Although transfection of GC-2 did result in expression of the highest number of receptors, all three CTR isoform-encoding cDNAs yielded very high levels of receptor expression that, in our experience, are above those necessary for maximal (saturation) levels of ligand-induced cAMP accumulation. Furthermore, binding affinity is independent of receptor number and the observed difference in maximal cAMP accumulation is still observed after normalization for transfection efficiency and the number of expressed receptors. Thus, the first intracellular domain sequences of a G protein–coupled receptor must interact directly or indirectly with a G protein, presumably G_s. We cannot exclude the possibility, however, that high levels of expression of either receptor isoform could result in the preferential binding of signaling proteins other than G_s (e.g., G_i or G_q) and thereby could alter the availability of such proteins in a way that potentiates the activation of adenylate cyclase in the GC-2–expressing cells.

Observations on other G protein–coupled receptors with seven transmembrane domains indicate that multiple intracellular domains contribute to functional G protein coupling (47–55). The third intracellular domain has been postulated to be the primary site of coupling to $G_{s\alpha}$ in some receptors (56), and several residues in this domain have been specifically implicated in G protein coupling (47–50, 57). This third intracellular loop shows considerable diversity in sequence among G protein–coupled receptors, however. CTRs possess an unusually short third intracellular loop. Such sequence divergence in the intracellular surfaces of these receptors has hindered the identification of universal G protein–coupling consensus sequences (57, 58). The second intracellular domain has also been implicated in G protein coupling in a large subgroup of receptors in the G protein–coupled receptor superfamily (47, 54, 55, 59). Moro et al. (55) proposed that a consensus sequence in the second intracellular domain of these receptors represents a major G protein–coupling site. The distinct family of receptors represented by the CTR does not contain this "consensus" sequence, however.

Mutagenesis experiments by Moro et al. (55) also suggested that the first intracellular domain of some receptors may be involved in coupling to G proteins that activate phospholipase C. Moro et al. (55) observed a ~ 50% reduction in phosphatidylinositol turnover resulting from a mutation introduced into the first intracellular domain of the muscarinic cholinergic receptor. We found that the insert in the first intracellular domain of the GC-10 CTR isoform resulted in a mean decrease in the CT-induced maximal cAMP response of ~ 66% compared with GC-2 (normalized for actual receptor number). The role of specific intracellular domains in coupling to different G proteins is of particular interest since the CTR couples to multiple signaling pathways (23, 24), possibly dependent upon the stage of the cell cycle (60).

We have not identified the functional significance of the 71-bp 5′-inserted sequence in the o-hCTR cDNA that encodes for 18 additional amino acids in the NH_2-terminal portion of the o-hCTR receptor. The scanning model of Kozak (46, 61) for initiation of mRNA translation predicts that preinitiation complexes rarely or never pass AUG codons with an A in the minus 3 position, such as exists in the o-hCTR 5′-AUG codon. This analysis, together with the observations reported in this paper that apparent CTR-encoding mRNA splice variants exist in which the 5′-initiation codon is deleted, suggests that translation of the o-hCTR isoform starts at the first (5′-) AUG. The cloned rat brain CTRs (29, 30) include two potential initiation codons 5′-to the single AUG found in the cDNAs encoding the porcine renal and GCT-CTR isoforms, suggesting the possibility of additional variants. The middle AUG of the rat brain CTR cDNAs is in a position homologous to that of the 5′-AUG in the o-hCTR. The cloned mouse CTR cDNA (11), like the o-hCTR, includes one additional 5′-initiation codon homologous to the middle AUG in the rat clones. Rodent receptors with 5′-regions homologous to the GCT and porcine renal CTRs that possess only a single start site have not yet been described.

The NH_2-terminal 18 amino acids encoded by the 5′-initiation codon of the o-hCTR does not contain a continuous stretch of hydrophobic amino acids flanked by polar residues and therefore is probably not a membrane-spanning domain or a signal recognition sequence (62). The 22–amino acid sequence following the second methionine (3′-AUG) does contain such a hydrophobic sequence consistent with those found in signal peptides (62). Since the porcine renal cell and GCT-CTRs can be expressed in COS cells, the more 3′-start codon can encode functional receptors. These facts do not exclude the 5′-AUG as a possible translation start site for the o-hCTR isoform, however. The additional 18 amino acids encoded by the 5′-initiation codon, together with the following 22 amino acids, could represent a bipartite leader sequence that might function, for example, in processes involved in subcellular protein targeting or trafficking. Bone and kidney CTRs are targeted to the basolateral surface of the osteoclast and certain renal tubule cells, respectively (63). Perhaps the truncated leader sequences of the bone GCT and porcine renal CTR isoforms result in the sorting of these CTRs to the basal or basolateral surfaces of the cells in which they are natively expressed. The putative bipartite leader of the o-hCTR may direct this protein to other more or less specific subcellular locations. The sequences responsible for the sorting of certain proteins to the apical or basolateral cell surface of MDCK kidney epithelial cells are in the NH_2-terminal domains of these proteins (64, 65) and other receptors that span the membrane seven times are targeted to specific subcellular locations in the development of specialized cells (66).

The predicted structure of the o-hCTR is most consistent with a protein with seven transmembrane domains and a cleaved signal sequence based on the earlier hydropathy models of von Heijne and Kyte-Doolittle (62). The more recent analysis of von Heijne and others, as applied in the new TopPred II software using the "GES" hydropathy scale and default parameters, is

also consistent with a membrane topology model with eight transmembrane domains (43). In this model, the uncleaved hydrophobic central portion of the 22-amino acid signal sequence would double as a stop-transfer membrane anchor and constitute the first transmembrane helical domain as well as a signal recognition sequence. The additional NH_2-terminal 18 amino acids encoded by the first (5′-) AUG would then constitute part of an uncleaved cytosolic tail. Such a receptor would possess eight transmembrane domains with the NH_2 and COOH termini both residing in the intracellular compartment. Further experiments are required to establish the actual configuration of the CTR proteins in the membrane, the structure of their NH_2-terminal domains, and the functional significance of any difference in these domains.

In summary, we have demonstrated the presence of two skeletal CTR isoform-encoding cDNAs from GCT and compared them with a third CTR isoform-encoding cDNA previously isolated from an ovarian carcinoma cell line. Expression of these three receptor isoforms in COS cells and parallel comparisons of ligand binding and ligand-dependent cAMP responses revealed that the first intracellular domain of the CTR is important in the modulation of receptor function and signaling.

Acknowledgments

This work was supported in part by U. S. Public Health Service grants AR-03564 (to S. M. Krane and S. R. Goldring), AR-07258 (to S. M. Krane), DK-46773 (to S. R. Goldring), AR-01895 (to A. H. Gorn), and a grant from the Paget Foundation (to S. R. Goldring).

References

1. Warshawsky, H., D. Goltzman, M. F. Rouleau, and J. J. M. Bergeron. 1980. Direct in vivo demonstration by radioautography of specific binding sites for calcitonin in skeletal and renal tissues of the rat. *J. Cell Biol.* 85:682–694.

2. Friedman, J., and L. G. Raisz. 1965. Thyrocalcitonin: inhibitor of bone resorption in tissue culture. *Science (Wash. DC).* 150:1465–1467.

3. Fischer, J. A., P. H. Tobler, M. Kaufmann, W. Born, H. Henke, P. E. Cooper, S. M. Sagar, and J. B. Martin. 1981. Calcitonin: regional distribution of the hormone and its binding sites in the human brain and pituitary. *Proc. Natl. Acad. Sci. USA.* 78:7801–7805.

4. Goltzman, D. 1985. Interaction of calcitonin and calcitonin gene-related peptide at receptor sites in target tissues. *Science (Wash. DC).* 227:1343–1345.

5. Fouchereau-Peron, M., M. S. Moukhtar, A. A. Benson, and G. Milhaud. 1981. Characterization of specific receptors for calcitonin in porcine lung. *Proc. Natl. Acad. Sci. USA.* 78:3973–3975.

6. Nicholson, G. C., C. S. D'Santos, T. Evans, J. M. Moseley, B. E. Kemp, V. P. Michelangeli, and T. J. Martin. 1988. Human placental calcitonin receptors. *Biochem. J.* 250:877–882.

7. Gorn, A. H., H. Y. Lin, M. Yamin, P. E. Auron, M. R. Flannery, D. R. Tapp, C. A. Manning, H. F. Lodish, S. M. Krane, and S. R. Goldring. 1992. Cloning, characterization and expression of a human calcitonin receptor from an ovarian carcinoma cell line. *J. Clin. Invest.* 90:1726–1735.

8. Chausmer, A., C. Stuart, and M. Stevens. 1980. Identification of testicular cell plasma membrane receptors for calcitonin. *J. Lab. Clin. Med.* 96:933–938.

9. Silvestroni, L., A. Menditto, G. Frajese, and L. Gnessi. 1987. Identification of calcitonin receptors in human spermatozoa. *J. Clin. Endocrinol. Metab.* 65:742–746.

10. Lin, H. Y., T. L. Harris, M. S. Flannery, A. Aruffo, E. H. Kaji, A. Gorn, L. F. Kolakowski, Jr., H. F. Lodish, and S. R. Goldring. 1991. Expression cloning of an adenylate cyclase-coupled calcitonin receptor. *Science (Wash. DC).* 254:1022–1024.

11. Yamin, M., A. H. Gorn, M. R. Flannery, N. A. Jenkins, D. J. Gilbert, N. G. Copeland, D. R. Tapp, S. M. Krane, and S. R. Goldring. 1994. Cloning and characterization of a mouse brain calcitonin receptor cDNA and mapping of the calcitonin receptor gene. *Endocrinology.* 135:2635–2643.

12. Jüppner, H., A.-B. Abou-Samra, M. Freeman, X.-F. Kong, E. Schipani, J. Richards, L. F. Kolakowski, Jr., J. Hock, J. T. Potts, Jr., H. M. Kronenberg, and G. V. Segre. 1991. A G protein-linked receptor for parathyroid hormone and parathyroid hormone-related peptide. *Science (Wash. DC).* 254:1024–1026.

13. Ishihara, T., S. Nakamura, Y. Kaziro, T. Takahashi, K. Takahashi, and S. Nagata. 1991. Molecular cloning and expression of a cDNA encoding the secretin receptor. *EMBO (Eur. Mol. Biol. Organ.) J.* 10:1635–1641.

14. Ishihara, T., R. Shigemoto, K. Mori, K. Takahashi, and S. Nagata. 1992. Functional expression and tissue distribution of a novel receptor for vasoactive intestinal polypeptide. *Neuron.* 8:811–819.

15. Jelinek, L. J., S. Lok, G. B. Rosenberg, R. A. Smith, F. J. Grant, S. Biggs, P. A. Bensch, J. L. Kuijper, P. O. Sheppard, C. A. Sprecher, et al. 1993. Expression cloning and signalling properties of the rat glucagon receptor. *Science (Wash. DC).* 259:1614–1616.

16. Thorens, B. 1992. Expression cloning of the pancreatic β cell receptor for the gluco-incretin hormone glucagon-like peptide 1. *Proc. Natl. Acad. Sci. USA.* 89:8641–8645.

17. Mayo, K. E. 1992. Molecular cloning and expression of a pituitary-specific receptor for growth hormone-releasing hormone. *Mol. Endocrinol.* 6:1734–1744.

18. Lin, C., S.-C. Lin, C.-P. Chang, and M. G. Rosenfeld. 1992. Pit-1-dependent expression of the receptor for growth hormone releasing factor mediates pituitary cell growth. *Nature (Lond.).* 360:765–768.

19. Spengler, D., C. Waeber, C. Pantaloni, F. Holsboer, J. Bockaert, P. H. Seeburg, and L. Journot. 1993. Differential signal transduction by five splice variants of the PACAP receptor. *Nature (Lond.).* 365:170–175.

20. Chen, R., K. A. Lewis, M. H. Perrin, and W. W. Vale. 1993. Expression cloning of a human corticotropin-releasing-factor receptor. *Proc. Natl. Acad. Sci. USA.* 90:8967–8971.

21. Usdin, T. B., E. Mezey, D. C. Button, M. J. Brownstein, and T. I. Bonner. 1993. Gastric inhibitory polypeptide receptor, a member of the secretin-vasoactive intestinal peptide receptor family, is widely distributed in peripheral organs and the brain. *Endocrinology.* 133:2861–2870.

22. Reagan, J. D. 1994. Expression cloning of an insect diuretic hormone receptor. *J. Biol. Chem.* 269:9–12.

23. Force, T., J. V. Bonventre, M. R. Flannery, A. H. Gorn, M. Yamin, and S. R. Goldring. 1992. A cloned porcine renal calcitonin receptor couples to adenylyl cyclase and phospholipase *C. Am. J. Physiol.* 262:F1110–F1115.

24. Chabre, O., B. R. Conklin, H. Y. Lin, H. F. Lodish, E. Wilson, H. E. Ives, L. Catanzariti, B. A. Hemmings, and H. R. Bourne. 1992. A recombinant calcitonin receptor independently stimulates 3′,5′-cyclic adenosine monophosphate and Ca^{2+}/inositol phosphate signaling pathways. *Mol. Endocrinol.* 6:551–556.

25. Abou-Samra, A.-B., H. Jppner, T. Force, M. W. Freeman, X.-F. Kong, E. Schipani, P. Urena, J. Richards, J. V. Bonventre, J. T. Potts, Jr., et al. 1992. Expression cloning of a common receptor for parathyroid hormone and parathyroid hormone-related peptide from rat osteoblast-like cells: a single receptor stimulates intracellular accumulation of both cAMP and inositol triphosphates and increases intracellular free calcium. *Proc. Natl. Acad. Sci. USA.* 89:2732–2736.

26. Zolnierowicz, S., P. Cron, S. Solinas-Toldo, R. Fries, H. Y. Lin, and B. A. Hemmings. 1994. Isolation, characterization, and chromosomal localization of the porcine calcitonin receptor gene: identification of two variants of the receptor generated by alternative splicing. *J. Biol. Chem.* 269:19530–19538.

27. Dal Torso, R., B. Sommer, M. Ewert, A. Herb, D. B. Pritchett, A. Bach, B. D. Shivers, and P. H. Seeburg. 1989. The dopamine D_2 receptor: two molecular forms generated by alternative splicing. *EMBO (Eur. Mol. Biol. Organ.) J.* 8:4025–4034.

28. Okamoto, N., S. Hori, C. Akazawa, Y. Hayashi, R. Shigemoto, N. Mizuno, and S. Nakanishi. 1994. Molecular characterization of a new metabotropic glutamate receptor mGluR7 coupled to inhibitory cyclic AMP signal transduction. *J. Biol. Chem.* 269:1231–1236.

29. Albrandt, K., E. Mull, E. M. G. Brady, J. Herich, C. X. Moore, and K. Beaumont. 1993. Molecular cloning of two receptors from rat brain with high affinity for salmon calcitonin. *FEBS (Fed. Eur. Biochem. Soc.) Lett.* 325:225–232.

30. Sexton, P. M., S. Houssami, J. M. Hilton, L. M. O'Keeffe, R. J. Center, M. T. Gillespie, P. Darcy, and D. M. Findlay. 1993. Identification of brain isoforms of the rat calcitonin receptor. *Mol. Endocrinol.* 7:815–821.

31. Oursler, M. J., P. Collin-Osdoby, F. Anderson, L. Ling, D. Webber, and P. Osdoby. 1991. Isolation of avian osteoclasts: improved techniques to preferentially purify viable cells. *J. Bone Miner. Res.* 6:375–385.

32.Horton, M. A., D. Lewis, K. McNulty, J. A. S. Pringle, and T. J. Chambers. 1985. Human fetal osteoclasts fail to express macrophage antigens. *Br. J. Exp. Pathol.* 66:103–108.

33. Huvos, A. G. 1991. Giant-cell tumor of bone. In Bone Tumors. 2nd edition. W. B. Saunders, Philadelphia. 429–467.

34.Goldring, S. R., A. L. Schiller, H. J. Mankin, J.-M. Dayer, and S. M. Krane. 1986. Characterization of cells from human giant cell tumors of bone. *Clin. Orthop. Relat. Res.* 204:59–75.

35. Goldring, S. R., M. S. Roelke, K. K. Petrison, and A. K. Bhan. 1987. Human giant cell tumors of bone identification and characterization of cell types. *J. Clin. Invest.* 79:483–491.

36. Joyner, C. J., J. M. Quinn, J. T. Triffitt, M. E. Owen, and N. A. Athanasou. 1992. Phenotypic characterization of mononuclear and multinucleated cells of giant cell tumour of bone. *Bone Miner.* 16:37–48.

37. Byers, V. S., A. S. Levin, J. O. Johnston, and A. Hackett. 1975. Quantita-

tive immunofluorescence studies of the tumor antigen-bearing cell in giant cell tumor of bone and osteogenic sarcoma. *Cancer Res.* 35:2520–2531.

38. Grano, M., S. Colucci, M. De Bellis, P. Zigrino, L. Argentino, G. Zambonin, M. Serra, K. Scotlandi, A. Teti, and A. Zambonin Zallone. 1994. A new model for bone resorbtion study in vitro: human osteoclast-like cells from giant cell tumors of bone. *J. Bone Miner. Res.* 9:1013–1020.

39. Sambrook, J., E. F. Fritsch, and T. Maniatis. 1989. Molecular Cloning: A Laboratory Manual. 2nd edition. Cold Spring Harbor Laboratory, Cold Spring Harbor, NY. 1885 pp.

40. Dilworth, D. D., and J. R. McCarrey. 1992. Single-step elimination of contaminating DNA prior to reverse transcriptase PCR. *PCR Methods Appl.* 1:279–282.

41. Kretz, K. A., G. S. Carson, and J. S. O'Brian. 1989. Direct sequencing from low-melt agarose with Sequenase. *Nucleic Acids Res.* 17:5864.

42. Devereux, J., P. Haeberli, and O. Smithies. 1984. A comprehensive set of sequence analysis programs for the VAX. *Nucleic Acids Res.* 12:387–395.

43. Claros, M. G., and G. von Heijne. 1994. TopPred II: an improved software for membrane protein structure predictions. *Comp. Appl. Biosci.* 10:685–686.

44. Seed, B., and A. Aruffo. 1987. Molecular cloning of the CD2 antigen, the T-cell erythrocyte receptor, by a rapid immunoselection procedure. *Proc. Natl. Acad. Sci. USA.* 84:3365–3369.

45. Morton, C. C., I. R. Kirsch, R. Taub, S. H. Orkin, and J. A. Brown. 1984. Localization of the β-globin gene by chromosomal in situ hybridization. *Am. J. Hum. Genet.* 36:576–585.

46. Kozak, M. 1984. Compilation and analysis of sequences upstream from the translation start site in eukaryotic mRNAs. *Nucleic Acids Res.* 12:857–872.

47. O'Dowd, B. F., M. Hnatowich, J. W. Regan, W. M. Leader, M. G. Caron, and R. J. Lef kowitz. 1988. Site-directed mutagenesis of the cytoplasmic domains of the human β_2-adrenergic receptor: localization of regions involved in G protein-receptor coupling. *J. Biol. Chem.* 263:15985–15992.

48. Cotecchia, S., S. Exum, M. G. Caron, and R. J. Lef kowitz. 1990. Regions of the α_1-adrenergic receptor involved in coupling to phosphatidylinositol hydrolysis and enhanced sensitivity of biological function. *Proc. Natl. Acad. Sci. USA.* 87:2896–2900.

49. Lechleiter, J., R. Hellmiss, K. Duerson, D. Ennulat, N. David, D. Clapham, and E. Peralta. 1990. Distinct sequence elements control the specificity of G protein activation by muscarinic acetylcholine receptor subtypes. *EMBO (Eur. Mol. Biol. Organ.) J.* 9:4381–4390.

50. Cheung, A. H., R.-R. C. Huang, and C. D. Strader. 1992. Involvement of specific hydrophobic, but not hydrophilic, amino acids in the third intracellular loop of the β-adrenergic receptor in the activation of G_s. *Mol. Pharmacol.* 41:1061–1065.

51. Konig, B. A., J. H. Arendt, M. McDowel, P. A. Kahlert, P. A. Hargrave, and K. P. Hoffmann. 1989. Three cytoplasmic loops of rhodopsin interact with transducin. *Proc. Natl. Acad. Sci. USA.* 86:6878–6882.

52. Dalman, H. M., and R. R. Neubig. 1991. Two peptides from the α_{2A}-adrenergic receptor alter receptor G protein coupling by distinct mechanisms. *J. Biol. Chem.* 266:11025–11029.

53. Okamoto, T., Y. Murayama, Y. Hayashi, M. Inagaki, E. Ogata, and I. Nishimoto. 1991. Identification of a G_s activator region of the β_2-adrenergic receptor that is autoregulated via protein kinase A-dependent phosphorylation. *Cell.* 67:723–730.

54. Weiss, E. R., D. J. Kelleher, and G. L. Johnson. 1988. Mapping sites of interaction between rhodopsin and transducin using rhodopsin antipeptide antibodies. *J. Biol. Chem.* 263:6150–6154.

55. Moro, O., J. Lameh, P. Hogger, and W. Sadee. 1993. Hydrophobic amino acid in the i2 loop plays a key role in receptor-G protein coupling. *J. Biol. Chem.* 268:22273–22276.

56. Luttrell, L. M., J. Ostrowski, S. Cotecchia, H. Kendall, and R. J. Lefkowitz. 1993. Antagonism of catecholamine receptor signaling by expression of cytoplasmic domains of the receptors. *Science (Wash. DC).* 259:1453–1457.

57. Okamoto, T., and I. Nishimoto. 1992. Detection of G protein-activator regions in M4 subtype muscarinic, cholinergic and α-adrenergic receptors based upon characteristics in primary structure. *J. Biol. Chem.* 267:8342–8346.

58. Voss, T., E. Wallner, A. P. Czernilofsky, and M. Freissmuth. 1993. Amphipathic α-helical structure does not predict the ability of receptor-derived synthetic peptides to interact with guanine nucleotide binding regulatory proteins. *J. Biol. Chem.* 268:4637–4642.

59. Munch, G., C. Dees, M. Hekman, and D. Palm. 1991. Multisite contacts involved in coupling of the β-adrenergic receptor with the stimulatory guanine-nucleotide-binding regulatory protein. *Eur. J. Biochem.* 198:357–364.

60. Chakraborty, M., D. Chatterjee, S. Kellokumpu, H. Rasmussen, and R. Baron. 1991. Cell cycle-dependent coupling of the calcitonin receptor to different G proteins. *Science (Wash. DC).* 251:1078–1082.

61. Kozak, M. 1981. Possible role of flanking nucleotides in recognition of the AUG initiator codon by eukaryotic ribosomes. *Nucleic Acids Res.* 9:5233–5252.

62. von Heijne, G. 1987. Sequence Analysis in Molecular Biology. Treasure Trove or Trivial Pursuit. Academic Press Inc., Orlando, FL. 188 pp.

63.Azria, M. 1989. The Calcitonins: Physiology and Pharmacology. Karger, Basel, Switzerland. 152 pp.

64. Roth, M. G., D. Gundersen, N. Patil, and E. Rodriguez-Boulan. 1987. The large external domain is sufficient for the correct sorting of secreted or chimeric influenza virus hemagglutinins in polarized monkey kidney cells. *J. Cell Biol.* 104:769–782.

65. Compton, T., I. E. Ivanov, T. Gottlieb, M. Rindler, M. Adesnik, and D. Sabatini. 1989. A sorting signal for the basolateral delivery of the vesicular stomatitis virus (VSV) G protein lies in its luminal domain: analysis of the targeting of VSV G-influenza hemagglutinin chimeras. *Proc. Natl. Acad. Sci. USA.* 86:4112–4116.

66. Nomura, A., R. Shigemoto, Y. Nakamura, N. Okamoto, N. Mizuno, and S. Nakanishi. 1994. Developmentally regulated postsynaptic localization of a metabotropic glutamate receptor in rat rod bipolar cells. *Cell.* 77:361–369.